Inhomogeneous tachyon condensation

JHEP06(2009)050

(http://iopscience.iop.org/1126-6708/2009/06/050)

Published by IOP Publishing for SISSA

Received: *March 10, 2009*
Revised: *May 15, 2009*
Accepted: *May 24, 2009*
Published: *June 15, 2009*

Inhomogeneous tachyon condensation

Mark Hindmarsh and Huiquan Li

Department of Physics and Astronomy, University of Sussex, Brighton BN1 9QH, U.K.

E-mail: m.b.hindmarsh@sussex.ac.uk, h.li@sussex.ac.uk

Abstract: We investigate the spacetime-dependent condensation of the tachyon in effective field theories. Previous work identified singularities in the field which appear in finite time: infinite gradients at the kinks, and (in the eikonal approximation) caustics near local minima. By performing a perturbation analysis, and with numerical simulations, we demonstrate and explain key features of the condensation process: perturbations generically freeze, and minima develop singular second derivatives in finite time (caustics). This last feature has previously been understood in terms of the eikonal approximation to the dynamics. We show explicitly from the field equations how this approximation emerges, and how the caustics develop, both in the DBI and BSFT effective actions. We also investigate the equation of state parameter of tachyon matter showing that it is small, but generically non-zero. The energy density tends to infinity near field minima with a charateristic profile. A proposal to regulate infinities by modifying the effective action is also studied. We find that although the infinities at the kinks are successfully regularised in the time-dependent case, caustics still present.

Keywords: Tachyon Condensation, D-branes

doi:10.1088/1126-6708/2009/06/050

JHEP06(2009)050

Contents

JHEP06(2009)050

1 Introduction

In Type II string theories, unstable branes of dimension p decaying into the stable ones with lower dimensions is well described by the Dirac-Born-Infeld (DBI) type effective action [1–3]:

$$S = -\int d^{p+1}x V(T)\sqrt{1+y}, \tag{1.1}$$

where $y = \eta^{\mu\nu}\partial_\mu T \partial_\nu T$, $V(T)$ is the asymptotic potential, and we use units in which $\alpha' = 1$. At the beginning of the condensation, the system has zero tachyon field $T = 0$ and is located on the top of the potential $V(T)$. It is unstable and will roll down when driven by a small perturbation. The field evolves towards the minimum of the potential $V = 0$, and the condensation ends. The final state corresponds to the disappearance of the unstable branes, replaced by "tachyon matter" whose properties are not well-understood.

The condensation process in the inhomogeneous case has also been studied. It has been realised that the equation of motion from the DBI action leads to solitonic solution with kinks and anti-kinks [4–7]. At the kinks and anti-kinks, the field remains zero, and become daughter branes of one dimension lower at the end of the condensation. While the field in between them grows with time and tends to infinity. The huge difference of the field values between these two areas makes the field gradient at kinks and anti-kinks very large and in fact, it can be semi-analytically shown to lead to infinity in finite time [7, 8]. The existence of this kind of singularity prevents straightforward numerical integration of the space-time dependent field equation [9, 10].

In between the kinks and anti-kinks where the field is approximately homogeneous, an eikonal approximation $1 + y = 0$ reveals that the second and higher derivatives of the field can reach infinity in finite time. This is interpreted as the formation of caustics [9].

The potential application of the tachyon condensation in the inflation scenario has been investigated, despite the various problems [11–16]. In the tachyon inflation model, agreement with the observational data can be achieved [17]. A complex tachyon field can produce cosmic strings after inflation [18–20]. The appearance of the pressureless tachyon matter at late stage of the condensation [3, 21] is also a feature of this model. The fluctuations of the tachyon matter in both the free and the expanding cosmology background [4, 14, 16, 17, 22] have been studied, and shown to increase linearly with time, just like ordinary pressureless matter.

In this paper, we study the condensation process using the field equations, demonstrating and explaining, both analytically and numerically, key features of the inhomogeneous tachyon condensation process. Perturbations around the homogeneous solutions $T = t$ "freeze", that is, show little change after a short initial relaxation period. What change there is reduces the curvature at maxima, and increases it at minima, until it becomes singular in finite time. This is interpreted as the formation of a caustic in the eikonal solution.

We also show explicitly from the field equations, backed up with numerical simulations, that the quantity $1 + y$ relaxes exponentially to zero, thus accounting for the accuracy of the eikonal equation.

We also investigate the energy density and pressure of condensing tachyon matter, showing that it is not quite pressureless, and that the energy density diverges in a characteristic $1/|\triangle x|$ form near the developing caustic.

One can ask if the instability is an artifact of the DBI effective action. To give a partial answer, we also study the boundary string field theory (BSFT) effective action [23, 24], showing that this approaches the eikonal equation eventually.

Finally, we show that a modification of the action proposed by [5] to regulate the gradient at a static kink does prevent the gradient of the field reaching infinity at the kinks in the time-dependent case, but does not prevent caustic formation between kinks.

The paper is constructed as follows. In section 2, we give the equation of motion and its solutions in simple cases. In section 3, we present the $1 + 1$ dimensional solutions near kinks and near extrema respectively. In section 4 and section 5, we discuss the dynamics approaching the vacuum respectively in the DBI and the BSFT effective theories. Based

JHEP06(2009)050

on the results, the features of the tachyon matter towards the end of condensation are investigated in section 6. In section 7, we discuss the generalised DBI action.

2 Equation of motion

From the DBI action (1.1), we can write down the equation of motion:

$$\left(\Box T - \frac{V'}{V}\right)(1+y) = \frac{1}{2}\partial^\mu T \partial_\mu (1+y), \tag{2.1}$$

where $\Box = \eta_{\mu\nu}\partial^\mu\partial^\nu$. An equivalent expression to the equation of motion is

$$\ddot{T} = f\left\{2\dot{T}\nabla_i\dot{T}\nabla^i T + (1+y)\nabla^2 T - \nabla_i T\nabla_j T\nabla^i\nabla^j T - \frac{V'}{V}(1+y)\right\}, \tag{2.2}$$

where $f = 1/(1+\nabla_i T\nabla^i T)$, $\nabla^2 = \partial_i\partial^i$ and $i, j = 1, \ldots, p$. $V(T)$ is the runaway tachyon potential and its field derivative is $V' = dV(T)/dT$. A suitable choice of potential, derived from the boundary conformal field theory on the worldsheet [25, 26], is

$$V = \frac{V_m}{\cosh(\beta T)}, \tag{2.3}$$

where V_m is the maximum potentail located at $T = 0$, and the constant $\beta = 1$ for the bosonic string and $\beta = 1/\sqrt{2}$ for superstring.

The energy-momentum tensor is:

$$T_{\mu\nu} = V(T)\left[\frac{\partial_\mu T\partial_\nu T}{\sqrt{1+\partial T\cdot\partial T}} - \eta_{\mu\nu}\sqrt{1+\partial T\cdot\partial T}\right]. \tag{2.4}$$

2.1 The static case

For the 1-dimensional static case, the solution to the field equation is most easily found by noting that conservation of energy-momentum requires that the pressure is constant:

$$T_{11} = \frac{-V}{\sqrt{1+T'^2}} = -V_0, \tag{2.5}$$

where $V_0 = V(T_0)$ is the minimum potential when the maximum field T_0 is achieved at $x = x_0$. The maximum field satisfies the condition $T'|_{T=T_0} = 0$.

For the inverse hyperbolic potential (2.3), the equation is solvable:

$$T(x) = \frac{1}{\beta}\sinh^{-1}\left[\sqrt{\frac{1}{r^2} - 1}\sin(\beta\triangle x)\right], \tag{2.6}$$

where $r = V_0/V_m$ and $\triangle x = x - x_m$. It represents an array of solitonic kinks and anti-kinks. Its gradient is:

$$T' = \pm\sqrt{\frac{1-r^2}{r^2 + \tan^2(\beta\triangle x)}}. \tag{2.7}$$

For fixed V_m, T' tends to infinity at kinks and anti-kinks, where $\triangle x = n\pi/\beta$, as $V_0 \to 0$, which is consistent with the slow motion analysis on the moduli space of [7].

2.2 The homogeneous case

In this case, the energy density is conserved and constant:

$$T_{00} = \frac{V}{\sqrt{1-\dot{T}^2}} = E, \tag{2.8}$$

which restricts $|\dot{T}| \leq 1$.

For the potential (2.3), the time dependent solution is:

$$T(t) = \begin{cases} \frac{1}{\beta}\sinh^{-1}[\sqrt{\frac{1}{l^2}-1}\cosh(\beta t)], & (E \leq V_m), \\ \frac{1}{\beta}\sinh^{-1}[\sqrt{1-\frac{1}{l^2}}\sinh(\beta t)], & (E > V_m), \end{cases} \tag{2.9}$$

and its time derivative is:

$$\dot{T} = \begin{cases} \pm\sqrt{\frac{l^2-1}{l^2-\tanh^2(\beta t)}}, & (E \leq V_m), \\ \pm\sqrt{\frac{1-l^2}{\coth^2(\beta t)-l^2}}, & (E > V_m), \end{cases} \tag{2.10}$$

where $l = E/V_m$. For $E > V_m$, $T = 0$, $|\dot{T}| = \sqrt{1-1/l^2}$ at $t = 0$ and $|T| \to \infty$, $|\dot{T}| \to 1$ as $t \to \infty$.

3 Solutions near kinks and extrema

In this section, we study the behaviour of solutions near stationary kinks and extrema, in order to gain insight into the singular dynamics, and to make contact with previous work [8, 9].

3.1 Around kinks

Following [8], we expand the field around a stationary kink or anti-kink located at $x = x_m$:

$$T(t,x) = a(t)\triangle x + \frac{1}{6}c(t)\triangle x^3 + \frac{1}{120}e(t)\triangle x^5 + \cdots, \tag{3.1}$$

where $\triangle x = x - x_m$.

For the potential (5.1), $V'/V = -\beta^2 T$. For the potential (2.3), $V'/V \simeq -\beta^2 T$ when $|T|$ is small. We use this relation and the expansion (3.1) in the field equation around kinks and anti-kinks, where $|T|$ is small. The comparison of coefficients gives the equation:

$$\ddot{a} = \beta^2 a + \frac{2a\dot{a}^2 + c}{1+a^2}. \tag{3.2}$$

We are more interested in the solution at late time when $a(t)$ becomes large. If we can neglect the contribution from $c(t)$,

$$\ddot{a}a = \beta^2 a^2 + 2\dot{a}^2. \tag{3.3}$$

To solve the equation, we set $a = 1/z$, giving

$$\ddot{z} + \beta^2 z = 0, \tag{3.4}$$

JHEP06(2009)050

with solution

$$z = z_1 \cos(\beta t) + z_2 \sin(\beta t). \tag{3.5}$$

By a suitable choice of the time coordinate, the solution of a can be written

$$a(t) = \frac{a_0}{\cos(\beta t)}, \tag{3.6}$$

where a_0 is constant. If we set $t_* = \pi/(2\beta)$, we approximately have: $a \sim 1/(t_* - t)$, which is consistent with the result of [8]. $a(t)$ grows to infinity in a finite time.

More precisely, we now also consider the evolution of the coefficient $c(t)$. With the same approximation of a being large, we can obtain the equation:

$$a^2\ddot{c} = 8a\dot{a}\dot{c} + (7\beta^2 a^2 - 6a\ddot{a})c - 6\beta^2 a\dot{a}^2 + e. \tag{3.7}$$

Combining this equation with eq. (3.3) and neglecting $e(t)$, we find

$$c(t) = -\beta^2 a = -\frac{\beta^2 a_0}{\cos(\beta t)}. \tag{3.8}$$

Therefore, the solution near the kinks and anti-kinks can be expressed as:

$$T(t,x) = a(t)\left[\triangle x - \frac{1}{6}\beta^2 \triangle x^3 + \cdots\right] \simeq \frac{a_0}{\beta}\frac{\sin(\beta \triangle x)}{\cos(\beta t)}. \tag{3.9}$$

This has the following properties at $x = x_m$: $T = 0$, $\dot{T} = 0$, $T'(t \to \infty) \to \infty$, $\ddot{T} = 0$ and $T'' = 0$, which are consistent with the discussion in section 2.

3.2 Around extrema

The field around a stationary peak or trough at $x = x_0$ satisfies the condition $T'|_{x=x_0} = 0$. The expansion around x_0 is written:

$$T(t,x) = T_0(t) + \frac{1}{2}b(t)\triangle x^2 + \frac{1}{24}d(t)\triangle x^4 + \cdots, \tag{3.10}$$

with $\triangle x = x - x_0$. For convenience, we only consider the behaviour around the field extrema whose values are positive $T_0(t) > 0$.

For the potential (2.3), $V'/V \simeq -\beta$ when T is positive. Inserting the expansion (3.10) in the field equation (2.2), we get:

$$\ddot{T}_0 = (\beta + b)(1 - \dot{T}_0^2). \tag{3.11}$$

The final value of $\dot{T}_0$ is decided by the relation between $b(t)$ and β. Here we only consider two special cases. When $b = -\beta$, $\dot{T}_0$ is constant and it corresponds to the static case. This is consistent to the static analytical solution (2.6), which has $T'' = -\beta$ at peaks. Secondly, if $|b| \ll \beta$, there is an explicit solution for $\dot{T}_0$

$$\dot{T}_0 = \tanh(\beta t). \tag{3.12}$$

The solution satisfies $\dot{T}_0 \in [0, 1]$. Otherwise, the solution can be formally expressed as: $\dot{T}_0 \simeq 1 - (A/2)e^{-2(\beta+b)t}$, where A is a small positive value.

JHEP06(2009)050

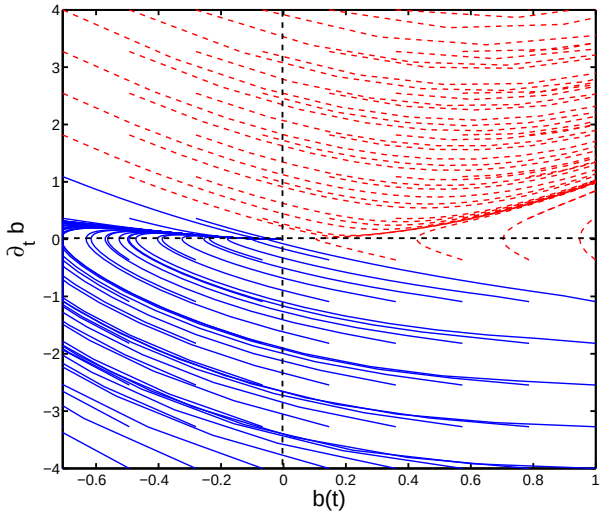

Figure 1. The time evolving curves of $\dot{b}(t)$ vs $b(t)$ with different initial values $(b_0, \dot{b}_0)$ in regions where $b \geq -\beta$. The blue, solid lines indicate that $b(t) \to 0$ at large t and the red, dashed lines indicate that $b(t)$ tends to infinity.

The equation for the coefficient $b(t)$ is:

$$\ddot{b} = 2\beta b^2 - 2(\beta - b)\dot{T}_0 \dot{b}. \tag{3.13}$$

Since we are considering the peaks on the positive field side $T_0 > 0$, $\dot{T}_0$ should be positive and tends to 1. Making use of the approximation $\dot{T}_0 \simeq 1$ for late time, eq. (3.13) can be rewritten as:

$$\partial_t(\dot{b} - b^2) = -2\beta(\dot{b} - b^2). \tag{3.14}$$

Hence,

$$\dot{b} = b^2 + C\exp(-2\beta t), \tag{3.15}$$

where $C = \dot{b}_0 - b_0^2$ is a constant, with $b_0 = b(t = 0)$ and $\dot{b}_0 = (db/dt)|_{t=0}$. We have made numerical solutions of (3.15). The distribution of the final values as a function of b_0 and $\dot{b}_0$ is presented in figure 1. From these results, we see that a peak ($b_0 < 0$) is most likely to flatten with time, but a trough ($b_0 > 0$) can deepen and become singular, and will always do so when $\dot{b}_0$ is positive. There is a sign of the developement of a caustic.

Let us just focus on the late time behaviour of $b(t)$. In terms of eq. (3.14), as $t \to \infty$ we will have

$$\dot{b} = b^2. \tag{3.16}$$

So the solution of b is

$$b(t) = \frac{b_0}{1 - b_0 t}, \tag{3.17}$$

where $b_0 = b(t = 0)$. Thus b blows up at $t = 1/b_0$ when $b_0 > 0$ while $b \to 0$ when $b_0 \leq 0$. But $\dot{b} \geq 0$ for both cases. This is consistent with the numerical solutions presented in figure 1.

JHEP06(2009)050

3.3 Caustics around extrema

In terms of the relations in eq. (3.12) and (3.15), we can estimate the quantity $1+y$ at late time as:

$$1+y \simeq 1-\dot{T}_0^2-\left(\dot{b}-b^2\right)\triangle x^2 \simeq \left(Ae^{-2bt}-C\triangle x^2\right)e^{-2\beta t}, \tag{3.18}$$

If $b>-\beta$, we see that $1+y\to 0$, as first noted in [9]. If we are in the region $\dot{b}<b^2$, C is negative and $1+y$ approaches zero from above.

Based on this relation, the authors of [9] argue that there should be caustics forming around the peaks or troughs. They rewrite the relation (3.18) as an eikonal equation:

$$\dot{S}^2-S'^2=1, \tag{3.19}$$

with the approximation $S\simeq T$ and develop a series of characteristic equations for (3.19) to give

$$S''(t,x)=\frac{S''(0,x)}{1-\frac{S''(0,x)}{(1+S'^2(0,x))^{3/2}}t}. \tag{3.20}$$

Thus S'' blows up in a finite time $t=(1+S'^2(0,x))^{3/2}/S''(0,x)$ when $S''(0,x)>0$, which is interpreted as the appearance of caustics or regions where the tachyon field becomes multivalued. We also note that when $S''(0,x)\leq 0$ there are no caustics, with $S''(t,x)\to 0$ as $t\to\infty$.

Our results are consistent with the eikonal analysis above: caustics form near troughs ($b>0$) in a time b_0^{-1}, where $b_0\simeq S''(0,x)$ at a trough, and peaks tend to flatten ($b\to 0$).

4 Perturbations

In this section, we will consider the evolution of perturbations around a condensing homogeneous tachyon field in an arbitrary dimensional Dp-brane. This will also approximately describes the evolution of the field between well-separated kinks and anti-kinks. A general form is:

$$T(t,x^i)=T_0(t)+\tau(t,x^i), \tag{4.1}$$

where $\tau(t,x^i)$ is the small perturbation along all spatial directions x^i $(i=1,\cdots,p)$ on the Dp-brane.

A trivial case is: $T_0(t)=0$. Around $T_0(t)=0$, $-V'/V\simeq\beta^2\tau$ for both potentials (2.3) and (5.1). Inserting $T(t,x^i)=\tau(t,x^i)$ in the field equation (2.2), we can get the perturbation equation:

$$\nabla^2\tau-\ddot{\tau}+\beta^2\tau=0, \tag{4.2}$$

as expected for a tachyon field with mass squared $-\beta^2$.

JHEP06(2009)050

4.1 Linear perturbations around a condensing field

Plugging the ansatz (4.1) in the field equation with the hyperbolic potential (2.3), we have the equation of τ

$$\begin{aligned}\left[\ddot{T}_0-\beta\left(1-\dot{T}_0^2\right)\right]+\left[\ddot{\tau}+2\beta\dot{T}_0\dot{\tau}-\left(1-\dot{T}_0^2\right)\nabla^2\tau\right]+,\\ \left[\beta\dot{\tau}^2-\left(\beta-\ddot{T}_0\right)\nabla\tau\cdot\nabla\tau-2\dot{T}_0\left(\nabla\tau\cdot\nabla\dot{\tau}-\dot{\tau}\nabla^2\tau\right)\right]\\ -\left[\left(\partial\tau\cdot\partial\tau\right)\Box\tau-\partial_\mu\tau\partial_\nu\tau\partial^\mu\partial^\nu\tau\right]=0.\end{aligned} \tag{4.3}$$

Solving the zeroth order equation covered in the first square bracket, we get the solution $\dot{T}_0=\tanh(\beta t)$, as given in eq. (3.12).

We first consider the linear perturbation covered in the second square bracket. This situation applies if all the first order terms remain dominating compared to the second order terms, though this is always not true as we can see later.

The solution of τ in the second square bracket is separate, and writing $\tau(t,x)=f(t)g(x)$, and we find:

$$\begin{cases}\nabla^2 g+k^2 g=0,\\ \ddot{f}+2\beta\tanh(\beta t)\dot{f}+k^2\mathrm{sech}^2(\beta t)f=0,\end{cases} \tag{4.4}$$

where $k^2=k_ik^i$ and k^i are arbitrary constants.

By making the reparameterisation

$$\rho=\frac{1}{1+e^{-2\beta t}},\ \left(\tfrac{1}{2}\leq\rho\leq 1\right), \tag{4.5}$$

we can rewrite the second equation in eq. (4.4) as

$$\rho(1-\rho)\frac{d^2f}{d\rho^2}+\kappa^2 f=0. \tag{4.6}$$

where $\kappa^2=\kappa_i\kappa^i$ and $\kappa_i=k_i/\beta$. It is a typical hypergeometric differential equation. The equation has two linearly independent solutions, the simpler one of which is given as [27]

$$f(t)=\rho(t)\,{}_2F_1\left(\frac{1-\sqrt{1+4\kappa^2}}{2},\frac{1+\sqrt{1+4\kappa^2}}{2};2;\rho(t)\right), \tag{4.7}$$

where ${}_2F_1$ is the hypergeometric function.

We will focus on the late time behaviour of τ when $\dot{T}_0$ is closed to 1. In this situation, the second equation in eq. (4.4) becomes $\ddot{f}+2\beta\dot{f}+4k^2\exp(-2\beta t)f=0$. With the reparameterization $\eta=\exp(-2\beta t)$, we have:

$$\eta\frac{d^2f}{d\eta^2}+\kappa^2 f=0. \tag{4.8}$$

The equation is a Bessel style differential equation [28]. Its solution is given as a conbination of two Bessel functions. The whole solution at late time can be expressed as:

$$\tau(t,x^i)=\int\frac{d^pk}{(2\pi)^p}\left[\tau_1(k_i)h^{(1)}(t,k)e^{ik_ix^i}+\tau_2(k_i)h^{(2)}(t,k)e^{-ik_ix^i}\right], \tag{4.9}$$

where $\tau_1(k_i)$, $\tau_2(k_i)$ are constant parameters corresponding to the mode k_i and

$$h^{(1,2)}(t,k) = e^{-\beta t} H_1^{(1,2)}\left(2\kappa e^{-\beta t}\right). \tag{4.10}$$

$H_1^{(1,2)}(s)$ are Hankel functions, which are linear combinations of the Bessel function of the first kind $J_1(s)$ and the second kind $Y_1(s)$: $H_1^{(1)}(s) = J_1(s) + iY_1(s)$ and $H_1^{(2)}(s) = J_1(s) - iY_1(s)$. They satisfy $H_1^{(1)}(s) = H_1^{(2)}(s)^*$. In order to get $\tau = \tau^*$, $\tau_1(k_i) = \tau_2(k_i)^*$. Then we can set $\tau_1(k_i) = \tau_0(k_i)e^{i\delta(k_i)}$ and $\tau_2(k_i) = \tau_0(k_i)e^{-i\delta(k_i)}$.

Since we are considering the real tachyon field T, the perturbation (4.9) should be real as well and can be expressed as, denoting $s = 2\kappa e^{-\beta t}$:

$$\tau(t,x^i) = \int \frac{d^p k}{(2\pi)^p} \frac{s}{2\kappa} \tau_0(k_i) \left[J_1(s)\cos\left(k_i x^i + \delta(k_i)\right) - Y_1(s)\sin\left(k_i x^i + \delta(k_i)\right)\right]. \tag{4.11}$$

For small parameters $0 < s \ll \sqrt{2}$,

$$J_1(s) \simeq \frac{s}{4}, \quad Y_1(s) \simeq -\frac{2}{\pi s}. \tag{4.12}$$

Thus, at late time, eq. (4.11) approximately reduces to:

$$\tau \simeq \frac{\beta}{\pi} \int \frac{d^p k}{(2\pi)^p} \frac{\tau_0(k_i)}{k} \sin\left(k_i x^i + \delta(k_i)\right). \tag{4.13}$$

This result indicates that the perturbation corresponding to each mode k_i freezes at late time and that shorter wavelength modes are damped more than longer wavelength.

4.2 Comparison with the numerical simulations

We make numerical simulations of the perturbations in $1+1$ dimensions based on the Hamiltonian formalism [3, 29, 30]. Define the momentum conjugate to T

$$\Pi = \frac{\delta S}{\delta \dot{T}} = \frac{V(T)\dot{T}}{\sqrt{1+y}}. \tag{4.14}$$

Then the equations of motion can be expressed as

$$\dot{\Pi} = \nabla^j \left(\frac{\nabla_j T \sqrt{\Pi^2 + V^2}}{\sqrt{1+(\nabla T)^2}}\right) - \frac{VV'\sqrt{1+(\nabla T)^2}}{\sqrt{\Pi^2+V^2}}, \tag{4.15}$$

$$\dot{T} = \frac{\Pi\sqrt{1+(\nabla T)^2}}{\sqrt{\Pi^2+V^2}}. \tag{4.16}$$

The simulation is implemented on a spatial lattice of 1280 points. The lattice spacing and the timestep are set to be respectively: $\delta x = 0.05$ and $\delta t = 0.01$. We use the symmetric difference for the first order field derivatives and a 3-point stencil for the second order field derivatives. We adopt the second order Runge-Kutta method for the time update. In the simulation, the constant $\beta = 1/\sqrt{2}$.

To get the perturbation, we first need to produce two sets of simulation data with two different initial conditions respectively: $T(t=0,x) = D$ and $T(t=0,x) = D + \delta(x)$, where

JHEP06(2009)050

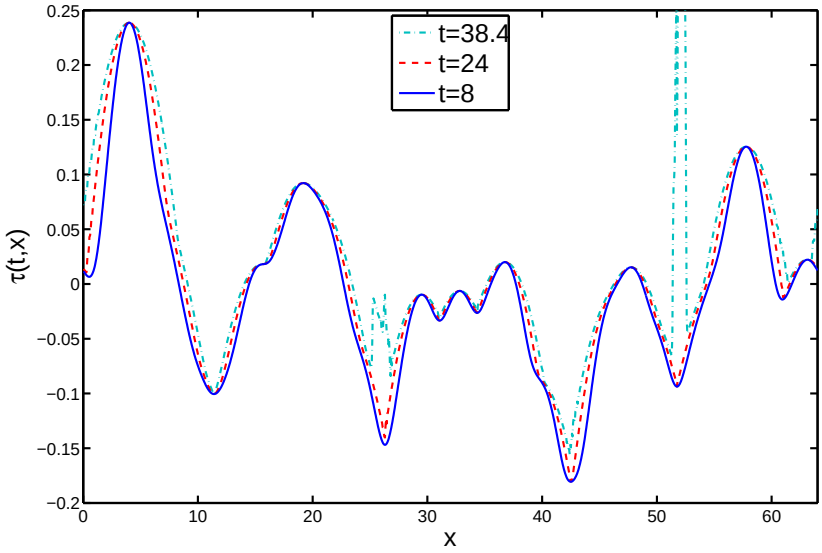

Figure 2. The numerical plots of the perturbation $\tau(t, x)$ based on eqs. (4.15) and (4.16). The initial homogeneous field is set to be $D = 1$.

D is the field value at $t = 0$: $D = T_0(t = 0)$, and $\delta(x)$ is the random initial perturbation: $\delta(x) = \tau(t = 0, x)$. The difference between them gives the $1 + 1$ dimensional evolution surface of $\tau(t, x)$. In figure 2, we present the plots of the perturbation at $t = 8, 24, 38.4$ respectively. We can see that the perturbation almost "freezes", especially at peaks and troughs, which is consistent with the linear perturbation analysis in the previous subsection. However, the second derivative $\nabla^2\tau$ can be seen to decrease in magnitude near peaks, and increase near troughs, until the simulation breaks down (signalled by spikes in τ at around $x \simeq 27$ and $x \simeq 53$). These features are consistent with the analysis in section 3, but not with the predictions from the linear perturbation equation. Hence, we need to take into account higher order perturbation terms to understand this behaviour.

4.3 Non-linear perturbations and development of caustics

We start with a discussion of the behaviour of $1 + y$. For large T, we can assume that $\dot{T} \to 1$, $\ddot{T} \to 0$ and $V'/V \simeq -\beta$. The equation of motion (2.1) becomes

$$\frac{\partial}{\partial t}(1 + y) \simeq -2\left(\nabla^2 T + \beta\right)(1 + y) + 2\nabla_i T \nabla_j T \nabla_i \nabla_j T - \dot{T}\frac{\partial}{\partial t}\left(\nabla^2 T\right). \tag{4.17}$$

If the last two terms are negligible compared to the first one, then $1 + y$ should decrease exponentially with time to zero. This accounts for the numerical observation first made in [9].

To check the expectation that $1 + y$ tends to zero exponentially, we present the plots of $1 + y$ in figure 3 for a field $T(t, x) = D + t + \tau(t, x)$, where the plots of the perturbation τ are given in figure 2. The result indicates that $1 + y$ really decreases with time to very small positive values exponentially in the early stage. However, the simulation can not

JHEP06(2009)050

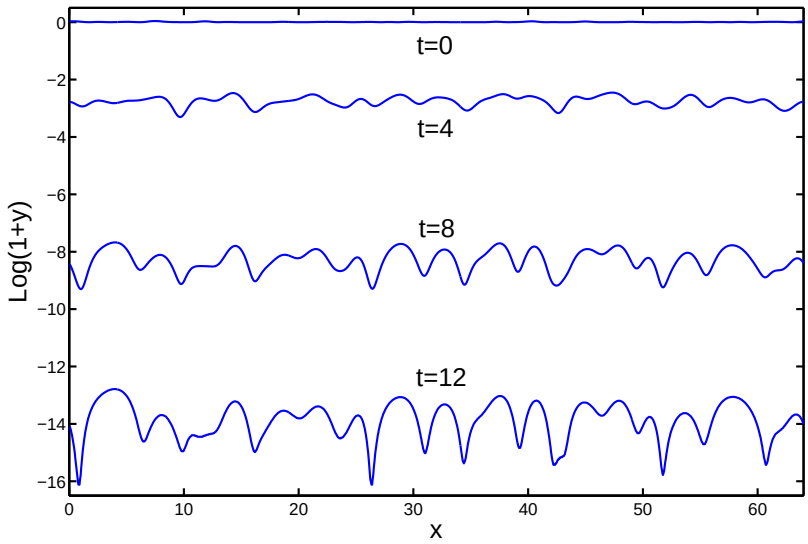

Figure 3. The plots of $\log(1+y)$ for the field $T(t,x) = D + t + \tau(t,x)$, where $D = 1$ and the plots of $\tau(t,x)$ are given in figure 2.

continue to late time due to instabilities emerging at the positions where τ eventually gets discontinous in figure 2, i.e., near troughs. This implies that the instability should correlate with the caustics formation. In what follows, we will determine how this happens in the perturbation method .

Including the quadratic order terms of τ in the second square bracket in eq. (4.3), we have in the limit $\dot{T}_0 \to 1$

$$\partial_t \left[2\dot{\tau} - (\nabla\tau)^2\right] = -\beta \left[2\dot{\tau} - (\nabla\tau)^2\right] + \ddot{\tau} - \dot{\tau}\left(2\nabla^2\tau + \beta\dot{\tau}\right). \tag{4.18}$$

It is consistent with eq. (3.14) if we set $\tau = b(t)\triangle x^2/2$ in $p = 1$ case. When the last two terms on the right hand side of the equation are less important than the first one, we will get at late time

$$1 + y \simeq 2\dot{\tau} - (\nabla\tau)^2 = 0. \tag{4.19}$$

Specially, $\dot{\tau} = 0$ when $\nabla_i\tau = 0$, i.e., at exactly the peaks or troughs, the perturbation "freezes". But away from the peaks and troughs, the perturbation increases with a increasing rate equal to $(\nabla\tau)^2/2$.

Let us see what features we can get from the equation $\dot{\tau} = (\nabla\tau)^2/2$ around peaks and troughs. Since τ "freezes" at exactly the peaks and troughs and grows away from them, the field gradient $|\nabla_i\tau|$ decreases near peaks and increases near troughs. Therefore, the curves of τ tend to flatten near peaks untill $\nabla_i\tau = 0$, where $\dot{\tau} = 0$ and so τ stops growing. Whereas near troughs, the curves of τ sharpen, with $|\nabla_i\tau|$ increasing. This accelerates the growth of τ. In this case, τ, $|\nabla_i\tau|$ and $\nabla^2\tau$ all will tend to infinity, which accounts for the caustic formation and so the instability near the vacuum.

JHEP06(2009)050

5 The BSFT action

The effective action derived from BSFT is given by [23, 24]: $\mathcal{L} = -V(T)F(y)$ with the potential

$$V(T) = \exp\left(-\frac{\beta^2 T^2}{2}\right), \tag{5.1}$$

and the kinetic part

$$F(y) = \frac{1}{2}\frac{4^y y\Gamma^2(y)}{\Gamma(2y)} = 2^{2y-1} yB(y), \tag{5.2}$$

where $y = \partial^\mu T\partial_\mu T$ as before and $B(y)$ is the beta function. It is easy to see that $F \geq 0$ when $y \geq -1/2$. Aspects of the dynamics arising from the the BSFT action have been given in [31, 32].

Using $\Gamma(1+u) = u\Gamma(u)$, we can derive the recursion relation

$$B(y) = 2^{2m}\frac{(y+\frac{2m-1}{2})(y+\frac{2m-3}{2})\cdots(y+\frac{1}{2})}{(y+m-1)(y+m-2)\cdots(y+1)y}B(y+m),\ m = 1, 2, 3, \ldots \tag{5.3}$$

From Stirling's approximation, $B(u) \simeq 2^{1-2u}\sqrt{\pi/u}$ for large u. Then the BSFT action can be expressed as

$$F(y) \simeq \frac{(y+\frac{2m-1}{2})(y+\frac{2m-3}{2})\cdots(y+\frac{1}{2})}{(y+m-1)(y+m-2)\cdots(y+1)}\sqrt{\frac{\pi}{y+m}}, \tag{5.4}$$

and we will find it useful to take $m \gg -y$.

For $m = 1$, we approximately have

$$F(y) \simeq \sqrt{\pi}\sqrt{1+y}, \tag{5.5}$$

when $1 + y \gg 1$. This is the DBI action. So the behaviour of the BSFT action (5.2) for large $1 + y$ should be similar to that discussed in previous sections. In what follows, we will discuss the behaviour near the vacuum when y is small or negative.

5.1 Time evolution

We first explore the homogeneous approach to the vacuum. The equation of motion in this case is

$$F - 2yF' = \frac{E}{V}, \tag{5.6}$$

where $y = -\dot{T}^2$, $F' = \partial F/\partial y$ and E is a constant.

The condensation starts with a small velocity $|\dot{T}|$. Let us consider the case when $\dot{T} = 0$. With the relation of the gamma function $\Gamma(2u) = 2^{2u-1}\Gamma(u)\Gamma(u+1/2)/\sqrt{\pi}$, we can rewrite the kinetic part $F(y)$ as

$$F(y) = \sqrt{\pi}\frac{\Gamma(y+1)}{\Gamma(y+\frac{1}{2})}. \tag{5.7}$$

Thus, $F(0) = 1$ since $\Gamma(1/2) = \sqrt{\pi}$. This gives $V(T) = E$ at $\dot{T} = 0$ in terms of the equation of motion.

Now we need to find where the tachyon potential gets the minimum value $V(T) = 0$, which corresponds to the vacuum. Since $y = -\dot{T}^2 \leq 0$ in the homogeneous case, we can change the action to the form by using $\Gamma(1-u)\Gamma(u) = \pi/\sin(\pi u)$

$$F(y) = -2^{2y+1}\pi \cot(\pi y)\frac{1}{B(-y)} \simeq -\sqrt{\pi}\cot(\pi y)\sqrt{-y}. \tag{5.8}$$

Then the homogeneous equation of motion (5.6) becomes

$$\frac{2(-\pi y)^{\frac{3}{2}}}{\sin^2(\pi y)} \simeq \frac{E}{V}. \tag{5.9}$$

It is easily seen that $V = 0$ at $y = -n$, where $n = 1, 2, 3, \ldots$. The behaviour in taking the limit $\dot{T}^2 \to n$ is,

$$V(T) \sim \frac{E}{2}\sqrt{\frac{\pi}{n^3}}(\dot{T}^2 - n)^2. \tag{5.10}$$

The equation implies that the tachyon potential vanishes for either $\dot{T}^2 \to n$ or $n \to \infty$. We will assume that only the first pole ($y = -1$) in eq. (5.9) is relevant, as the condensation starts with $y \simeq 0$.

5.2 Dynamics near the vacuum

The full equation of motion for a general $F(y)$ is

$$\left(2\frac{F''}{F'}\partial_\mu T\partial_\nu T + \eta_{\mu\nu}\right)\partial^\mu\partial^\nu T + \frac{V'}{V}\left(y - \frac{1}{2}\frac{F}{F'}\right) = 0. \tag{5.11}$$

Note that $V' = \partial V/\partial T$, $F' = \partial F/\partial y$ and $F'' = \partial^2 F/\partial y^2$.

We now consider the dynamics approaching the vacuum when $y \to -1$ from above. Since $F/F' = 1/(\ln F)'$ and $F''/F' = (\ln F)''/(\ln F)' + (\ln F)'$, we only need to know $(\ln F)'$ and $(\ln F)''$ for deriving the equation of motion. In the limit $y \to -1$, we approximately have for any $m \geq 2$ from eq. (5.4)

$$(\ln F)' \sim -\frac{1}{1+y}, \quad (\ln F)'' \sim \frac{1}{(1+y)^2}. \tag{5.12}$$

The corresponding expressions for the DBI action are $(\ln F)' = 1/[2(1+y)]$ and $(\ln F)'' = -1/[2(1+y)^2]$. Inserting them in the equation of motion, we have

$$\left(\Box T - \frac{V'}{V}\right)(1+y) \simeq 2\partial^\mu T\partial_\mu(1+y), \tag{5.13}$$

So it is very similar to eq. (2.1) for the DBI action. The only difference is a change of the coefficient on the right hand side. Therefore, there should be similar consequences for the dynamics approaching the vacuum from the BSFT action to those from the DBI action. That is, the perturbations "freeze" and the second derivative becomes discontinuous.

JHEP06(2009)050

6 Tachyon matter

Reverting to the DBI action, the energy density and the pressure are given in flat spacetime by eq. (2.4):

$$\rho = T_{00} = \frac{1+(\nabla T)^2}{\sqrt{1+y}} V(T), \tag{6.1}$$

$$p_i = T_{ii} = -V(T)\frac{1+y-(\nabla_i T)^2}{\sqrt{1+y}} = q + \frac{(\nabla_i T)^2}{1+(\nabla T)^2}\rho, \tag{6.2}$$

where there is no sum on i and $q = \mathcal{L} = -V(T)\sqrt{1+y}$, and so

$$w_i = \frac{p_i}{\rho} = -\frac{1+y}{1+(\nabla T)^2} + \frac{(\nabla_i T)^2}{1+(\nabla T)^2}. \tag{6.3}$$

From the above formulas, it is easy to see that the system at the beginning of the tachyon condensation has positive energy density and negative pressure everywhere: $p_i = -\rho = -V_m$, the characteristic of the interior of a brane. After the condensation starts, the behavior in different areas becomes different.

Consider the case that the decay of the Dp-brane happens only in the x^1 direction to produce a D$(p-1)$-brane. Then the decay process can be described by a kink-anti-kink tachyon solution along the x^1 direction.

First, we consider the appearance of a D$(p-1)$-brane, which we locally choose to be orthogonal to the x^1-direction. Since $\dot{T} = 0$ and $|\nabla_1 T| \to \infty$ towards the end of the decay at kinks, the energy density near the kinks $\rho_K \to \infty$. If the approximate solution found in section 3.1 is to be believed, this divergence happens in finite time, in accordance with the analysis in the string field theory [33, 34]. The pressure components in all p spatial directions are respectively: $p_{jK} = q$ $(2 \le j \le p)$ and

$$p_{1K} = p_{jK} + \frac{(\nabla_1 T)^2}{1+(\nabla_1 T)^2}\rho_K. \tag{6.4}$$

Therefore, $p_{jK} \simeq -\rho_K$ and $p_{1K} \simeq p_{jK} + \rho_K$ near the end of the condensation. And so $p_{jK} \to -\infty$ and $p_{1K} \to 0$ as $t \to \infty$, which further give $w_{jK} \to -1$ and $w_{1K} \to 0$. This is consistent with the appearance of a D$(p-1)$-brane in a vacuum.

Second, we consider the approach to vacuum of a homogeneous field with an expanded inhomogeneous part. The energy density ρ_V and the pressure p_{iV} near the vacuum can be analysed using the results in section 3. The final values of ρ_V and p_{iV} at the end of the condensation are not obviously determined because the two quantities $V(T)$ and $1+y$ both tend to zero as $t \to \infty$. They can be estimated in terms of the expression of $1+y$ in eq. (3.18), from which we see that $1+y \simeq Ae^{-2(\beta+b)t} \to Ae^{-2\beta t}$ when $b < 0$ (e.g., near peaks) and $1+y \to -C\triangle x^2 e^{-2\beta t}$ when $b > 0$ (e.g., near troughs). To keep $1+y$ positive, we assume that $C = \dot{b}_0 - b_0^2$ is negative. For the hyperbolic potential (2.3), $V(T) \simeq 2V_m \exp[-\beta(D+t)]$. Thus the energy density near the vacuum is

$$\rho_V \simeq \begin{cases} \frac{2V_m}{\sqrt{A}} e^{-\beta D}, & (b<0), \\ \frac{2V_m(1+b^2\triangle x^2)}{\sqrt{Ae^{-2bt}-C\triangle x^2}} e^{-\beta D}, & (b>0). \end{cases} \tag{6.5}$$

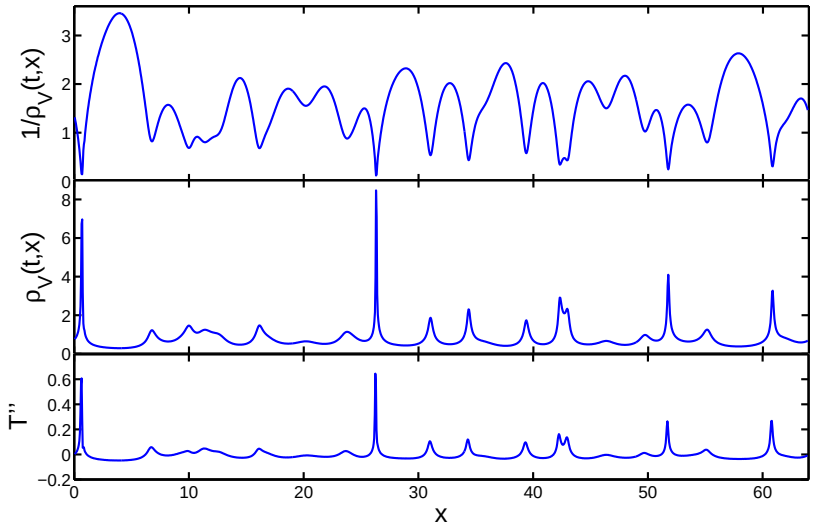

Figure 4. The correlation between the energy density $\rho_V(t,x)$ near the vacuum and the second derivative T''. The plots are made at $t = 16$. It is easily seen that $\rho_V(t,x)$ peaks at positions where T'' also peaks and that $1/\rho_V \sim |\triangle x|$ near the peaks of ρ_V.

The energy density tends to a constant near peaks and diverges at troughs $\triangle x = 0$ as $t \to \infty$. When b is not too large, $\rho_V \sim 1/|\triangle x|$ near but away from the trough at $\triangle x = 0$.

In figure 4, we present the plots of the energy density ρ_V and its inverse $1/\rho_V$ relative to the plots of the second derivative $b = T''$ at a time $t = 16$. The figure indicates strong relation between ρ_V and T'': the energy density peaks where T'' also peaks. By comparison with figure 2, we see that the sharpest peaks in T'' occur at troughs in T. The top plot shows evidence that around the peaks of the energy density, we have the approximate relation $1/\rho_V \sim |\triangle x|$.

It is interesting to note that the tachyon fluid is not quite pressureless in general. Indeed, from eq. (6.2), noting that $q \to 0$ near the vacuum as $t \to \infty$, we find ρ_V: $p_{iV} \sim \rho_V(\nabla_i T)^2/[1 + (\nabla T)^2]$. Given that T "freezes", we see that the small fluctuations give rise to a small pressure. The equation of state parameter w_{iV} is non-zero.

7 The generalised DBI action

The problem with the divergence in the gradient of the field near kinks has been recognised for some time [8–10], and regularisations of the action have been proposed in [5, 35] with respect to this problem, which have the important property that their static kinks have finite field gradients as the minimum potential $V_0 \to 0$. In what follows, we will consider the modified action given in [5] in the $1 + 1$ dimensions:

$$\mathcal{L} = -V(T)(1 + y)^{\frac{1}{2}(1+\epsilon)}. \tag{7.1}$$

where ϵ is a small positive value. The equation of motion from it is:

$$\ddot{T} = f\{2\left(1-\epsilon^2\right)\dot{T}\nabla_i T\nabla^i\dot{T} - \frac{V'}{V}(1+y)(1-\epsilon y) \\ +(1+\epsilon)[(1+y)\nabla^2 T - (1-\epsilon)\nabla_i T\nabla_j T\nabla^i\nabla^j T]\}, \tag{7.2}$$

where $f = 1/\left[(1+\epsilon)(1+\nabla_i T\nabla^i T - \epsilon\dot{T}^2)\right]$.

First, we consider the field expansion around the kinks and antikinks in the case of the hyperbolic potential (2.3). Doing the field expansion like (3.1), we get the equation of $a(t)$:

$$\ddot{a} = \frac{\beta^2 a}{1+\epsilon} - \frac{\epsilon\beta^2 a^3}{1+\epsilon} + \frac{(1-\epsilon)(2a\dot{a}^2+c)}{1+a^2} + \epsilon c. \tag{7.3}$$

So when a grows large and satisfies $1 \ll a \ll 1/\sqrt{\epsilon}$, we have a similar solution to eq. (3.6). When $a \gg 1/\sqrt{\epsilon}$, the a^3 term becomes important and a begins to execute damped oscillations. a settles to $a = 1/\sqrt{\epsilon}$.

To show this point clearly, we can transform eq. (7.3) into a soluble form, assuming $1 + a^2 \simeq a^2$, and neglecting c. When $\epsilon \neq 1/2$, we set $a = z^{-1/(1-2\epsilon)}$ and then have:

$$\ddot{z} + \frac{\partial \mathrm{U}(z)}{\partial z} = 0, \tag{7.4}$$

where $\mathrm{U}(z)$ is:

$$\mathrm{U}(z) = \frac{\left(\frac{1}{2}-\epsilon\right)\beta^2 z^2}{(1+\epsilon)}\left[1 + \left(\frac{1}{2}-\epsilon\right) z^{-\frac{2}{1-2\epsilon}}\right], \tag{7.5}$$

For $\epsilon > 0$, the minimum value of $\mathrm{U}(z)$ happens at $z = \epsilon^{(1/2-\epsilon)}$ or

$$a = \frac{1}{\sqrt{\epsilon}}. \tag{7.6}$$

This value should be the final field gradient $T' \simeq a$ as $t \to \infty$. When $\epsilon = 1/2$, we can set $a = e^z$ and get the same equation as in (7.4) but with a different potential $\mathrm{U}(z)$:

$$\mathrm{U}(z) = \frac{\beta^2}{6}\left(e^{2z} - 4z\right). \tag{7.7}$$

The position according for the minimum potential $\mathrm{U}(z)$ is $z = \ln\sqrt{2}$ or $a = \sqrt{2}$, which is consistent to the above result of $\epsilon \neq 1/2$.

For the expansion around extrema, we get:

$$\ddot{T}_0 = \left[\frac{1+\epsilon\dot{T}_0^2}{1+\epsilon}\beta + b\right]\frac{1-\dot{T}_0^2}{1-\epsilon\dot{T}_0^2}. \tag{7.8}$$

When $\epsilon < 1$, $1 - \epsilon\dot{T}_0^2$ is always positive if $|\dot{T}_0| \leq 1$. Similar to the analysis for the DBI action with $\epsilon = 0$, $|\dot{T}_0|$ still goes to 1 here at the end of condensation.

With the approximation $\dot{T}_0 \simeq 1$ for positive T_0, the equation for $b(t)$ can be expressed as:

$$(1-\epsilon)\,\partial_t\left(\dot{b} - b^2\right) = -2\,(\beta - \epsilon b)\,(\dot{b} - b^2). \tag{7.9}$$

JHEP06(2009)050

For $\epsilon < 1$, it can be shown both analytically and numerically that there are still two possible final values for $b(t)$ at $t \to \infty$. When b tends to zero, we can write the solution similar to (3.14). So it can evolve to zero at $t \to \infty$. When $b(t \to \infty) \to \infty$, b grows to infinity more quickly than the case with $\epsilon = 0$. Thus caustics are possible to form in a finite time for the modified DBI action.

Hence, although this modified effective action solves the problem of diverging gradients near kinks, it still has unstable solutions and breaks down as the vacuum is approached.

8 Conclusions

We have investigated the inhomogeneous tachyon condensation process, focusing on the solutions near kinks (where $T = 0$) and also in regions where the field is approximately uniform.

We obtained an approximate spacetime-dependent solution near the kinks and antikinks, verifying that the spatial derivative of the field T' tends to infinity in a finite time. We show that this singularity can be avoided by modifying the effective action in $1 + 1$ dimensions, which is consistent with the result obtained in the static case by [5, 35].

We then studied inhomogeneous tachyon condensation in the absence of kinks. In (3.18), an analysis assuming that the tachyon field obeyed the eikonal equation $\dot{T}^2 + \nabla T^2 = 1$ showed that near troughs T'' diverges in finite time, which was interpreted as the production of caustics in free-streaming matter. Directly from the semi-analytical solutions, we learnt how the field obeys this equation and how the solutions from this equation lead to singularities in T''. A linear analysis shows that perturbations "freeze", except near extrema; Adding in higher order terms shows that the curvature ($\nabla^2 T$) increases near troughs (extrema with $\nabla^2 T > 0$) and decreases near peaks ($\nabla^2 T < 0$). For the former case, this leads to discontinuous gradients near troughs, which in the eikonal approximation leads to caustics. Moreover, the energy density ρ_V diverges as $t \to \infty$ near troughs. The pressure of tachyon matter is small, but the equation of state parameter w does not generically vanish.

The same analysis applies also to BSFT effective theories, and to another simple proposal for modifying the effective action [5, 35]. The large gradients and higher derivatives signal a breakdown of the effective action (1.1) for describing the dynamics of the tachyon field near the vacuum. Whether or not caustics actually form remains open for further discussion.

Acknowledgments

HL is supported by a Dorothy Hodgkin Postgraduate Award.

References

[1] M.R. Garousi, *Tachyon couplings on non-BPS D-branes and Dirac- Born-Infeld action*, *Nucl. Phys.* **B 584** (2000) 284 [hep-th/0003122] [SPIRES].

JHEP06(2009)050

[2] E.A. Bergshoeff, M. de Roo, T.C. de Wit, E. Eyras and S. Panda, *T-duality and actions for non-BPS D-branes*, *JHEP* **05** (2000) 009 [hep-th/0003221] [SPIRES].

[3] A. Sen, *Field theory of tachyon matter*, *Mod. Phys. Lett.* **A 17** (2002) 1797 [hep-th/0204143] [SPIRES].

[4] K. Hashimoto and N. Sakai, *Brane - antibrane as a defect of tachyon condensation*, *JHEP* **12** (2002) 064 [hep-th/0209232] [SPIRES].

[5] P. Brax, J. Mourad and D.A. Steer, *Tachyon kinks on non BPS D-branes*, *Phys. Lett.* **B 575** (2003) 115 [hep-th/0304197] [SPIRES].

[6] C.-j. Kim, Y.-b. Kim and C.O. Lee, *Tachyon kinks*, *JHEP* **05** (2003) 020 [hep-th/0304180] [SPIRES].

[7] M. Hindmarsh and H. Li, *Perturbations and moduli space dynamics of tachyon kinks*, *Phys. Rev.* **D 77** (2008) 066005 [arXiv:0711.0678] [SPIRES].

[8] J.M. Cline and H. Firouzjahi, *Real-time D-brane condensation*, *Phys. Lett.* **B 564** (2003) 255 [hep-th/0301101] [SPIRES].

[9] G.N. Felder, L. Kofman and A. Starobinsky, *Caustics in tachyon matter and other Born-Infeld scalars*, *JHEP* **09** (2002) 026 [hep-th/0208019] [SPIRES].

[10] N. Barnaby, A. Berndsen, J.M. Cline and H. Stoica, *Overproduction of cosmic superstrings*, *JHEP* **06** (2005) 075 [hep-th/0412095] [SPIRES].

[11] A. Mazumdar, S. Panda and A. Perez-Lorenzana, *Assisted inflation via tachyon condensation*, *Nucl. Phys.* **B 614** (2001) 101 [hep-ph/0107058] [SPIRES].

[12] M. Fairbairn and M.H.G. Tytgat, *Inflation from a tachyon fluid?*, *Phys. Lett.* **B 546** (2002) 1 [hep-th/0204070] [SPIRES].

[13] D. Choudhury, D. Ghoshal, D.P. Jatkar and S. Panda, *On the cosmological relevance of the tachyon*, *Phys. Lett.* **B 544** (2002) 231 [hep-th/0204204] [SPIRES].

[14] L. Kofman and A. Linde, *Problems with tachyon inflation*, *JHEP* **07** (2002) 004 [hep-th/0205121] [SPIRES].

[15] M. Sami, P. Chingangbam and T. Qureshi, *Aspects of tachyonic inflation with exponential potential*, *Phys. Rev.* **D 66** (2002) 043530 [hep-th/0205179] [SPIRES].

[16] G. Shiu and I. Wasserman, *Cosmological constraints on tachyon matter*, *Phys. Lett.* **B 541** (2002) 6 [hep-th/0205003] [SPIRES].

[17] D.A. Steer and F. Vernizzi, *Tachyon inflation: tests and comparison with single scalar field inflation*, *Phys. Rev.* **D 70** (2004) 043527 [hep-th/0310139] [SPIRES].

[18] G.R. Dvali and S.H.H. Tye, *Brane inflation*, *Phys. Lett.* **B 450** (1999) 72 [hep-ph/9812483] [SPIRES].

[19] S. Sarangi and S.H.H. Tye, *Cosmic string production towards the end of brane inflation*, *Phys. Lett.* **B 536** (2002) 185 [hep-th/0204074] [SPIRES].

[20] D. Choudhury, D. Ghoshal, D.P. Jatkar and S. Panda, *Hybrid inflation and brane-antibrane system*, *JCAP* **07** (2003) 009 [hep-th/0305104] [SPIRES].

[21] A. Sen, *Tachyon matter*, *JHEP* **07** (2002) 065 [hep-th/0203265] [SPIRES].

[22] A.V. Frolov, L. Kofman and A.A. Starobinsky, *Prospects and problems of tachyon matter cosmology*, *Phys. Lett.* **B 545** (2002) 8 [hep-th/0204187] [SPIRES].

JHEP06(2009)050

[23] D. Kutasov, M. Mariño and G.W. Moore, *Remarks on tachyon condensation in superstring field theory*, hep-th/0010108 [SPIRES].

[24] P. Kraus and F. Larsen, *Boundary string field theory of the DD-bar system*, *Phys. Rev.* **D 63** (2001) 106004 [hep-th/0012198] [SPIRES].

[25] D. Kutasov and V. Niarchos, *Tachyon effective actions in open string theory*, *Nucl. Phys.* **B 666** (2003) 56 [hep-th/0304045] [SPIRES].

[26] M. Smedback, *On effective actions for the bosonic tachyon*, *JHEP* **11** (2003) 067 [hep-th/0310138] [SPIRES].

[27] A. Jeffrey and D. Zwillinger, *Table of integrals, series, and products*, Academic Press (2007).

[28] M. Abramowitz and I. A. Stegun, *Handbook of mathematical functions with formulas, graphs, and mathematical tables*, ninth Dover Printing, tenth GPO Printing ed., Dover New York (1965).

[29] G.W. Gibbons, K. Hori and P. Yi, *String fluid from unstable D-branes*, *Nucl. Phys.* **B 596** (2001) 136 [hep-th/0009061] [SPIRES].

[30] G. Gibbons, K. Hashimoto and P. Yi, *Tachyon condensates, carrollian contraction of Lorentz group and fundamental strings*, *JHEP* **09** (2002) 061 [hep-th/0209034] [SPIRES].

[31] S. Sugimoto and S. Terashima, *Tachyon matter in boundary string field theory*, *JHEP* **07** (2002) 025 [hep-th/0205085] [SPIRES].

[32] N. Barnaby, *Caustic formation in tachyon effective field theories*, *JHEP* **07** (2004) 025 [hep-th/0406120] [SPIRES].

[33] A. Sen, *Rolling tachyon*, *JHEP* **04** (2002) 048 [hep-th/0203211] [SPIRES].

[34] F. Larsen, A. Naqvi and S. Terashima, *Rolling tachyons and decaying branes*, *JHEP* **02** (2003) 039 [hep-th/0212248] [SPIRES].

[35] E.J. Copeland, P.M. Saffin and D.A. Steer, *Singular tachyon kinks from regular profiles*, *Phys. Rev.* **D 68** (2003) 065013 [hep-th/0306294] [SPIRES].

JHEP06(2009)050